Published in final edited form as:
Neuromuscul Disord. 2012 July ; 22(7): 648–658. doi:10.1016/j.nmd.2012.03.002.

Myogenesis in dysferlin-deficient myoblasts is inhibited by an intrinsic inflammatory response

Tatiana V. Cohen, **Jonathan E. Cohen**, and **Terence A. Partridge***
Research Center for Genetic Medicine, Children's National Medical Center, 111 Michigan Avenue NW, Washington, DC 20010, USA

Abstract

Limb-girdle muscular dystrophy type 2B results from mutations in dysferlin, a membrane-associated protein involved in cellular membrane repair. Primary myoblast cultures derived from dysferlinopathy patients show reduced myogenic potential, suggesting that dysferlin may regulate myotube fusion and be required for muscle regeneration. These observations contrast with the findings that muscle develops normally in pre-symptomatic dysferlinopathy patients. To better understand the role of dysferlin in myogenesis, we investigated this process *in vitro* using cells derived from two mouse models of dysferlinopathy: SJL/J and A/J mice. We observed that myotubes derived from dysferlin-deficient muscle were of significantly smaller diameters, contained fewer myonuclei, and displayed reduced myogenic gene expression compared to dysferlin-sufficient cells. Together, these findings suggest that the absence of dysferlin from myoblasts is detrimental to myogenesis. Pro-inflammatory NFκB signaling was upregulated in dysferlin-deficient myotubes; the anti-inflammatory agent celastrol reduced the NFκB activation and improved myogenesis in dysferlin-deficient cultures. The results suggest that decreased myotube fusion in dysferlin deficiency is attributable to intrinsic inflammatory activation and can be improved using anti-inflammatory mediators.

Keywords

Muscular dystrophy; Inflammation; Thunder of God Vine; MyoD; p65/RelA; Immortomouse; Muscle culture

1. Introduction

Three clinically distinct myopathies are associated with mutations in the protein dysferlin [1]. Limb-girdle muscular dystrophy 2B (LGMD) is an autosomal recessive myopathy marked by proximal muscle weakness, with an onset in the late teens ([2,3]; reviewed in [4]). Myoshi myopathy features a progressive muscle wasting involving distal muscles, in particular, lower limbs with an earlier onset and necessity for a wheelchair within 10 years following the onset of disease ([5]; reviewed in [4]). A third related myopathy is a rapidly

*Corresponding author. Address: Research Center for Genetic Medicine, The George Washington University Medical Center, Children's National Medical Center, 111 Michigan Avenue, NW, Washington, DC 20010, USA. Tel.: +1 202 476 2562; fax: +1 202 476 6014. tpartridge@cnmcresearch.org (T.A. Partridge).

progressive severe weakness affecting distal anterior muscles [6]. These myopathies feature ongoing regeneration and fibrosis [7], a selective loss of type 2 muscle fibers with the extent of degeneration that is intermediate between Duchenne muscular dystrophy (DMD) and sarcoglycanopathy and a moderate degree of inflammation surrounding the necrotic fibers, in particular, overexpression of major histocompatibility complex class I [8].

The dysferlin gene, *DYSF*, encodes a 230 kDa membrane-bound protein, dysferlin [9], a member of the ferlin family of proteins which also includes otoferlin [10] and myoferlin [11]. Members of this protein family contain C2 domains, found in synaptotagmins, which interact with SNARE proteins, and mediate membrane vesicle trafficking [12]. Dysferlin has been proposed to play a role in membrane repair [13] and dysferlin-deficient muscle is slow to recover from contraction-induced injury [14].

Dysferlin transcript levels increase during myofusion in human muscle satellite cells [15,16] and protein accumulates at the site of fusing C2C12 myotubes, suggesting that dysferlin may play a role in myotube fusion [17]. Myoblasts obtained from patients carrying mutations in the dysferlin gene, showed defective myotube fusion potential when cultured *in vitro*, as well as delayed myogenin expression, suggesting a myotube differentiation delay [15]. Furthermore, the myogenin promoter was shown to be directly regulated by dysferlin and reduction of dysferlin by siRNA knockdown also reduced myogenin mRNA levels [15].

Dysferlin-deficient muscle is marked by inflammatory infiltrate. Recently the molecular complex known as the inflammasome which mediates innate immunity by promoting the maturation of inflammatory cytokine IL-1β, was shown to be upregulated in muscle lysates and myoblasts derived from SJL/J mice, a model for dysferlinopathy [18]. IL-1β binds to receptors that signal through the nuclear factor kappa-light-chain-enhancer of activated B cells (NFκB) pathway, central in regulating innate immunity, inflammation and apoptosis [19]. IL-1β receptor activation results in the activation of the IκB kinase (IKK), a complex composed of subunits IKKα, IKKβ and IKKγ. IKK then acts on a complex composed of the p65/p50 NFκB dimer and IκBα, which keeps NFκB in an inactive state. Phosphorylation of IκBα by IKK results in its rapid degradation and subsequent release of the p65/p50 NFκB dimer (reviewed in [25]), which allows it to translocate to the nucleus and transcriptionally activate target genes. Whereas NFκB is important for maturation of immune cells, it inhibits myogenesis in skeletal muscle [20]. NFκB inhibits myogenesis by regulating the YY1 transcriptional repressor ([21]; reviewed in [22]) and by posttranslationally inhibiting MyoD [23]. Inhibition of NFκB signaling by ablation of the p65 subunit of NFκB or deletion of IKKβ reduces inflammation and promotes skeletal muscle regeneration in *mdx* mice ([24]; reviewed in [25]). Furthermore, the glucocorticoid dexamethasone, via inhibition of NFκB, increases myogenic fusion efficiency in C2C12 cells and improves myotube formation in dysferlin-deficient cells [16].

In the present study, we examined myogenesis *in vitro* in myoblasts derived from two mouse models of dysferlin-deficiency. We show that murine dysferlin-deficient satellite cells fuse to form muscle fibers, but that the fibers are thinner, contain fewer myonuclei, and show decreased expression of myogenic genes and proteins. Dysferlin-deficient myoblasts also show intrinsically upregulated NFκB signaling. Suppression of the pro-inflammatory

signaling using a general NFκB and TNFα signaling blocker, celastrol, improved myogenesis in these cells, suggesting that the myogenesis defect is due to the activated NFκB inflammatory signaling.

2. Materials and methods

2.1. Mice

All mice were handled according to local Institutional Animal Care and Use Committee guidelines. Dysferlin-deficient SJL/J (JAX#000686), A/J, (JAX#000646), and C57Bl/ 6J (JAX#000664) mice were purchased from Jackson Laboratory (Bar Harbor, ME). The Immortomouse® (Charles River Labs, Wilmington, MA) mouse line harbors a transgene construct containing H-2K^b (MHC Class I antigen) 5′ promoter sequences fused to the early region of the temperature-sensitive SV40 Large T antigen mutant tsA58 [26]. Immortomice® were crossed with A/J mice [27] and genotyping was performed on F2 littermates using the following primers. Large T antigen forward: 5′-GAGTTTCATCC TGATAAAGGAGG-3′ and large T antigen reverse: 5′-G TGGTGTAAATAGCAAAGCAAGC-3′ and A/J wild-type forward 5′-TTCCTCTCTTGTCGGTC TAG-3′; wild-type/mutant reverse 5′-CTTCACTGG GAAGTATGTC G-3′ and mutant forward 5′-GCCTT GATCAGAGTAAC TGTC-3′ using 30 cycles of 94 °C denaturing, 59 °C annealing and 72 °C extension.

2.2. Cell culture

Primary satellite cells were derived from 3 month old SJL/J and C57Bl/6J mice. Hind-limb muscle was finely minced, then incubated in digestion buffer containing Dispase II (Sigma, St. Louis, MO), collagenase A (Roche Applied Science, Indianapolis, IN) and DNAse I (Sigma). The muscle homogenate was triturated and passed through progressively smaller cell strainers (100, 70 and 40 μm). Following each filtration, the muscle homogenate was centrifuged at 1200 rpm for 5 min and resuspended in PBS containing 0.1% BSA and 0.2% DNAse I. The isolated cells were plated at a density of 5×10^4 cells per well in Matrigel™ (BD Biosciences, Bedford, MA)-coated 6-well dishes and cultured in DMEM (Invitrogen, Carlsbad, CA) containing 20% fetal bovine serum (Invitrogen. Carlsbad, CA), 1% penicillin–streptomycin (Invitrogen) and 2 mM L-glutamine (Invitrogen) and 2% chick embryo extract (CEE, Accurate Chemical and Scientific Corp., Westbury, NY) (growth medium). This method resulted in a mixed culture containing approximately 10% satellite cells. Following 7 days in growth medium, myoblasts were induced to fuse into myotubes by switching the medium to DMEM containing 5% horse serum and 2% CEE (differentiation media) and incubating for 2 additional days.

Immortalized satellite cells were isolated from single muscle fibers of 6 weeks old A/J dysferin-deficient (A/J) or dysferlin-sufficient (WT) F2 littermates of A/J × Immortomouse® crosses as previously described [26]. Proliferating cells were maintained at 33 °C in growth medium containing 20 ng/ml final IFNγ (Millipore, Billerica, MA). To induce differentiation, cells were plated onto Matrigel™-coated dishes and cultured at 37 °C in differentiation media for 5 days. Cellular proliferation was determined using an MTT Cell Proliferation Kit I (Roche Applied Science) according to the manufacturer’s instructions.

2.3. Immunofluorescence

Myoblasts cultured on silanized coverslips were fixed with fresh 4% paraformaldehyde, blocked with 5% horse serum and 1% bovine serum albumin, and then incubated overnight with appropriate primary antibody. Fluorophore-conjugated secondary antibodies were applied for 1 h and the cells were imaged using an Apotome-outfitted Zeiss microscope equipped with a CCD camera or using a Zeiss LSM510 confocal microscope. The following antibodies were used: sarcomeric myosin heavy chain (MHC) (clone MF20; Developmental Studies Hybridoma Bank, Iowa City, IA) was used at 1:200; desmin (Abcam, Cambridge, MA), 1:200; MyoD (Vector, Burlingame, CA), 1:100; and calreticulin, 1:100 (Abcam). Following washes, cells were incubated with secondary antibodies Alexa Fluor 488 anti-rabbit and Alexa Fluor 568 anti-mouse (Invitrogen) at 1:300 dilution.

2.4. RNA isolation and real-time analysis

Total RNA was isolated from differentiating A/J and WT satellite cell lines ($n = 3$ independent clonal lines) using the RNeasy Mini Kit (Qiagen, Valencia, CA). First strand synthesis was performed using the First Strand cDNA Synthesis kit (Roche) according to manufacturer's instructions. Quantitative reverse transcription-polymerase chain reaction (qRT-PCR) was performed on an ABI 7900HT Fast Real-Time PCR System using SYBR® Green (Applied Bio-systems, Carlsbad, CA). Raw C_t values were normalized to S18 and GAPDH and relative gene expression was obtained using the $\Delta\Delta C_t$ method [28]. NFκB signaling was analyzed in differentiated myotubes using an 84-transcript NFκB Signaling Pathway PCR array (SABiosciences, Frederick, MD) according to the manufacturer's instructions.

2.5. Western blotting

Whole cell lysates were prepared using NP40 Lysis buffer (Invitrogen) according to manufacturer instructions. Protein concentration was determined using a Bio-Rad Microplate Protein Assay (Bio-Rad, Hercules, CA). Proteins were separated on a denaturing 4–12% Bis–Tris SDS–PAGE gel and transferred onto PVDF membranes. Following blocking with milk, membranes were immunoblotted with indicated antibodies. MyoD (Novus Biologicals, Littleton, CO) was used at 1:1000; phospho-p65, p105/p50, IKK (Cell Signaling Technologies, Danvers, MA) at 1:1000; and vinculin (Sigma, 1:10,000). After washing, membranes were probed with HRP-conjugated anti-rabbit or anti-mouse secondary antibody (1:5000 dilution; GE Healthcare, Piscataway, NJ). The membranes were incubated with ECL Western Blotting Substrate (Pierce, Rockford, IL) and processed on Bio-Lite X-ray film.

2.6. Data and statistical analysis

All values are reported as mean ± standard error of mean (SEM). Descriptive statistics, including two-tailed Student's *t*-test were used to assess statistical significance using Minitab (Minitab Inc., State College, PA) and Sigma Plot 10.0 software (SPSS, Chicago, IL). Normalized rank plots were created in Excel (Microsoft) using the RANK function by assigning a rank value to each measurement and normalizing to the total number of data

points. Image analysis of fluorescence and confocal images, including z-stacks was performed in ImageJ.

3. Results

3.1. Muscle cultures derived from SJL/J dysferlin-deficient mice form myotubes that are thinner than those from dysferlin-sufficient mice

The expression of dysferlin increases as myoblasts differentiate to form myotubes in culture. Conversely, the absence of dysferlin in human myoblasts diminishes myogenic potential resulting in lowered fusion indices, suggesting that dysferlin could be an important mediator of skeletal muscle differentiation [15]. In mouse models of dysferlinopathy, defective myofusion occurs in the absence of dysferlin [29]; however, *in vivo* regeneration does not appear to be compromised in dysferlin-deficient mouse muscle [30,31]. To reconcile these discrepancies we determined whether murine primary dysferlin-deficient myoblasts show any defect in myofusion and used primary muscle myoblasts derived from pre-symptomatic SJL/J mice. The SJL/J mutation results from a 146 bp genomic deletion containing a splice site in the intron between exons 45 and 46. The resultant SJL/J dysferlin transcript is shortened by 171 bp and dysferlin protein concentration is reduced to approximately 15% of levels in dysferlin-sufficient animals [32,33].

Muscle satellite cells were derived from SJL/J or control C57Bl/6J mice, cultured for 7 days in growth media, and differentiated for 2 days in fusion medium. Myotube cultures were immunostained with anti-desmin and anti-MyoD antibodies (Fig. 1A) or an anti-myosin heavy chain (MHC) antibody (Fig. 1B). Quantitation of myotube diameters showed that C57Bl/6J cells formed many large-diameter fibers. A cumulative frequency distribution was used to show a typical distribution with several large myotubes with diameters ranging from 30 to 50 μm and the rest ranging from 10 to 20 μm (mean = 18.6 ± 2.8 μm). The distribution for myotubes derived from SJL/J mice was shifted to the left due to decreased diameters and significantly fewer large-diameter fibers (mean = 12.8 ± 1.1 μm; $P = 0.031$) (Fig. 1C and D). Quantitation of myonuclear number showed a range from 2 to 35 (mean = 8.5 ± 2.0) whereas SJL/J fibers contained significantly fewer nuclei per fiber (mean = 3.3 ± 4.0; $P = 0.004$) (Fig. 1E and F). A linear relationship was found between fiber width and nuclear number indicating that decreased fiber diameters were not due to inability to grow but rather due to less efficient fusion in SJL/J (Fig. 1G). The fusion index was calculated using MHC and Hoechst staining, as defined by the percentage of nuclei in MHC+ve cells and myotubes compared to the total number of nuclei. The fusion index in wild-type cells was 43.7 ± 6.8% ($n = 226$ cells) and was significantly reduced in SJL/J myotubes at 9.2 ± 1.1% ($n = 202$ cells; $P < 0.05$) compared to respectively (Fig. 1H).

3.2. A/J dysferlin-deficient cells do not proliferate differently from dysferlin-sufficient cells but also form thinner myotubes

The observed myofusion defect could be due to the SJL/ J strain irrespective of dysferlin, or due to different contributions of non-muscle cells in the mixed-cell primary culture. In addition, the SJL/J mutation results in production of low levels of dysferlin (approximately 15% of controls [33]). Thus, we sought to characterize myofusion in another mouse model

of dysferlinopathy, the A/J mice, in which dysferlin protein is absent [27]. Furthermore, we sought to eliminate differences due to contaminating non-muscle cells by examining myoblast cultures derived from single immortalized satellite cells (H-2K) obtained from A/J dysferlin-deficient and -sufficient mice. We initially compared proliferation of H-2K myoblasts derived from dysferlin-deficient (A/J) or dysferlin-sufficient (WT) H-2K mice. Cells were plated at 5×10^4 per well in growth media and immunostained for MyoD to mark myogenic cells and a cytoplasmic marker, calreticulin (Fig. 2A). There were no significant differences in proliferation between dysferlin-deficient- and -sufficient myoblasts after 3 days in proliferation media; average cell numbers per field was 118.14 ± 5.83 for WT and 128.81 ± 8.07 for A/J; $P = 0.35$, $n = 3$ individual clone lines (Fig. 2B). We then measured the rate of cell proliferation by counting cells up to 5 days in culture. Similarly, there were no differences between dysferlin-deficient and -sufficient cells (Fig. 2C). To further validate these results, an MTT Cell Proliferation assay was used to show that growth rates were not different between dysferlin-deficient and -sufficient cells. These results suggest that myoblast proliferation was not affected by the absence of dysferlin.

We sought to determine if myogenic fusion is also affected in H-2K A/J dysferlin-deficient cells, similarly to SJL/J primary cultures. Cells were plated at 5×10^4 cells per well in 6-well dishes and allowed to differentiate for up to 5 days then immunostained with antibodies against MHC and, to mark unfused cells, calreticulin. As was observed with SJL/J primary myotubes, H-2K A/J myotubes appeared thinner than H-2K A/J dysferlin-sufficient myotubes (Fig. 3A). Quantitation of the fusion index showed that in WT cells, 47.2 ± 8.4% of the nuclei were in myotubes whereas in A/J cells, this number was significantly reduced to 13.2 ± 3.7% ($P < 0.05$), consistent with the SJL/J primary muscle cells (Fig. 3B). To ensure that the decrease in diameter size was not due to the poor attachment of the dysferlin-deficient myotubes to the substrate, we performed confocal imaging and acquired z-stacks of a small population of the fibers and analyzed the cross-sectional areas of five fields by an orthogonal view function in ImageJ (data not shown). From the fibers that were analyzed, no differences were observed in the cross-sectional areas of fibers containing an equal number of nuclei. In contrast, larger cross-sectional areas were observed in fibers containing a greater number of nuclei, indicating that only nuclear number (a measure of the number of fused cells), and not cytoplasmic content is the factor determining the decreased myotube diameter in dysferlin deficiency. These data suggest that myofusion is reduced but not eliminated in dysferlin-deficient murine muscle cells.

3.3. Myogenic transcripts are downregulated in dysferlin-deficiency

To determine whether myotubes with thinner diameters in dysferlin-deficiency also show a reduction of muscle-specific transcripts, we examined myotube cultures by qRT-PCR. Primary myoblasts were derived from hind-limb muscles of SJL/J or control (C57Bl/6J) mice. Cultured myoblasts were differentiated into myotubes and analyzed by qRT-PCR. Myotubes derived from SJL/J mice showed reduced expression of several muscle-specific genes including: *Myf*5, *Myod*, *Myog*, *Myh1* and *Ttn* (data not shown). We then examined the expression level of myogenic transcripts in cultured H-2K A/J myoblasts. Myoblasts were differentiated for up to 6 days in culture and transcript levels of *Myod*, *Myog*, *Myh1* and *Myh4* were measured by qRT-PCR. During the course of differentiation, *Myod* and *Myog*

transient gene expression increased first, between days 2 and 5, and was followed by the muscle structural genes, *Myh1* and *Myh4*, which increased between days 3 and 6. Quantitation of these transcripts in three independently-derived H-2K A/J clones showed lower expression of these muscle genes throughout the course of the differentiation period (Fig. 3C–F). To confirm whether decreased transcript levels of *Myod* also result in decreased MyoD protein expression, we examined whole cell lysates by Western blotting and observed a similar decrease in MyoD protein levels in lysates from H-2K A/ J dysferlin-deficient muscle cells compared with dysferlin-sufficient muscle cells (Fig. 3G).

3.4. Increased pro-inflammatory environment and gene expression of NFκB gene targets in dysferlin-deficient H-2K-A/J cells

We recently showed that the NALP-3 containing inflammasome is upregulated in dysferlinopathy patient and SJL/ J mouse muscle [18]. The upregulation of inflammation may activate the NFκB pathway in muscle, which could directly inhibit the activity of MyoD [24,25]. Thus, we profiled differentiated H-2K A/J muscle cells using an NFκB-specific qRT-PCR array. Of the 84 genes present on the array, 14 were significantly upregulated in dysferlin-deficient H-2K A/J cells (Table 1). There was upregulation of NFκB pathway genes *Ikbke* and *Nfkbia*. Moreover, the NFκB targets *Tlr9*, *Tnfsf14* and *Il1b* were significantly upregulated.

3.5. Celastrol decreases NFκB signaling and improves myogenesis in dysferlin-deficient H-2K myoblasts

Up-regulation of the NFκB pathway in muscle can directly inhibit the activity of MyoD [24,25] and thus result in defective myogenesis in A/J myoblasts. Thus, we tested whether inhibiting the NFκB signaling pathways using the anti-inflammatory agent celastrol might affect myogenesis in dysferlin-deficient cells. Celastrol was added to the cultures on day 1 of differentiation at concentrations ranging from 0.02 to 200 nM, previously shown to robustly inhibit NFκB signaling [34]. At these concentrations, cellular toxicity was not observed after 5 days in culture. Immunostaining the A/J cultures using an antibody that recognizes the phosphorylated p65/RelA subunit of NFκB showed increased p65/RelA in A/J cells (Fig. 4A). In wild-type cultures, some phosphorylated p65/RelA staining can be observed in cells associated with myofibers. In contrast, in A/J cultures, the p65/RelA staining is much brighter and localized to the nuclei. Treatment with 200 nM celastrol reduced the activated p65/RelA to levels that were barely detectable in both wild-type and A/J cultures. Western blotting further showed that phosphorylated p65/RelA was upregulated in dysferlin-deficient A/J cells compared with dysferlin-sufficient and treatment with celastrol inhibited p65/RelA activity to levels observed in wild-type myotubes, whereas total protein levels of p105, p50 and IKKαβ were not affected in the A/J myotube cultures (Fig. 4B).

To determine whether inhibition of NFκB signaling can also improve myogenesis, we measured the fusion index in wild-type and A/J cells that were incubated with 200 nM celastrol during days 2–5 of differentiation. We found that celastrol increased the fiber diameters of A/J myotubes (Fig. 4A). Quantification showed that the average number of nuclei that were in myotubes in wild-type cells was 27.0 ± 2.0% (SEM; $n = 3$ independent

experiments). Treatment with celastrol increased the average to 32.1 ± 1.2%. In A/J cells, the average number of nuclei in myotubes was 20.5 ± 2.0%, significantly lower than wild-type ($P < 0.05$) and treatment with celastrol significantly increased the fusion index of A/J cells to 29.4 ± 1.5% ($P < 0.01$) (Fig. 4C). The number of nuclei per fiber was also significantly affected by celastrol treatment. The average nuclear number in wild-type cells was 13.4 ± 1.7 and in celastrol-treated wild-type cells increased to 14.8 ± 1.8. The average nuclear number in A/J cells was significantly lower at 5.6 ± 0.5 ($P < 0.05$) and was increased to 9.0 ± 1.6 ($P < 0.05$) by celastrol treatment (Fig. 4D). In addition, treatment with celastrol increased transcript levels of *Myh4* and *Myog* in dysferlin-deficient A/J myotubes (data not shown). These data suggest that inhibition of NFκB signaling using celastrol can ameliorate the myofusion defect observed in dysferlin-deficient cultures.

4. Discussion

4.1. Activated pro-inflammatory networks inhibit myogenesis in dysferlin-deficient myoblasts

Inflammatory muscular dystrophies, DMD and LGMD2B, feature upregulation of pro-inflammatory molecular pathways, including activation of the NFκB pathway [25]. NFκB is a pleiotropic transcription factor activated during processes of inflammation and cancer, and linked to processes involving proliferation and apoptosis. NFκB is a dimer comprised of subunits p65/RelA and p50 (derived from the precursor protein p105). When inactive, the p65/p50 NFκB dimer is retained in the cytoplasm in a complex with the inhibitor protein IκBα. Pro-inflammatory cytokines such as TNFα or IL-1β released by macrophages and damaged myofibers lead to activation of the IκB kinase (IKK), a complex composed of subunits IKKα, IKKβ and IKKγ. IKK phosphorylates IκBα which results in its rapid degradation and subsequent release of the p65/ p50 NFκB dimer (reviewed in [25]). Released NFκB becomes phosphorylated on the p65 subunit and translocates to the nucleus where it transcriptionally activates target genes. NFκB has been shown to play a key role in negatively regulating myogenesis by interacting with the YY1 transcriptional repressor [21] and post-translationally inhibiting MyoD [23]. NFκB was previously shown to be upregulated in *mdx* mice [24]. In the present study, we found upregulated NFκB signaling in dysferlin-deficient cells, evident by enhanced phosphorylation of the p65 subunit and increased transcript levels of *Nfkie* and *Ikbke* as well as NFκB pathway target genes *Tlr9*, *Tnfsf14* and *Il1b*. These studies suggest that NFκB may be a common factor that mediates activated pro-inflammatory networks in both *mdx* and dysferlin-deficiency. Several lines of evidence suggest that upregulated NFκB signaling could negatively affect muscle regeneration in these inflammatory pathologies. Decreasing activated p65 using a haploinsufficient mouse model increases myoblast proliferation and myogenic index [35]. In the present study, inhibition of NFκB signaling using celastrol reduced the myogenic defect and increased myotubes diameters in dysferlin-deficiency. Consistently, inhibition of NFκB signaling using the glucocorticoid dexamethasone increases myofiber diameters in differentiating C2C12 cells [16], indicating that improved myogenesis is not a unique property of celastrol. Rather, together with previous reports, these data provide further support for inhibition of NFκB signaling to facilitate skeletal muscle regeneration during muscular dystrophy.

The results of the present study do not discount the contribution of other inflammatory networks activated in dysferlin-deficient cells. For example, thrombospondin 1 (TSP-1), a soluble factor involved in monocyte chemotaxis, was recently shown to be highly expressed in muscle cells derived from dysferlinopathy patients [36]. It may be that the activation of NFκB signaling, via induction of pro-inflammatory gene targets including *Il1b* and *Tnfsf14*, prepares muscle to facilitate the recruitment of macrophages *in vivo*, and is inhibitory for muscle regeneration until the underlying pathology is resolved.

4.2. Role of dysferlin in membrane repair and myotube fusion

Dysferlin contains Ca^{2+}-sensitive C2 domains also found in the synaptotagmins, the vesicle-associated proteins that regulate exocytosis and vesicle fusion [37]. Dysferlin-deficient muscle fibers show reduced ability to reseal in the presence of Ca^{2+} following membrane damage [13]. These observations are supported by an increasing number of reports implicating dysferlin in the process of membrane repair (reviewed in [38,39]). The exact mechanism by which dysferlin regulates membrane repair remains unclear, although it is hypothesized to act as a Ca^{2+} sensor during endocytosis-based membrane resealing. Whereas direct Ca^{2+} sensor activity has not been demonstrated for dysferlin, such activity is implicated by the homology of dysferlin with otoferlin, a ferlin expressed in inner hair cells that has been directly demonstrated to interact with SNAP-25 and syntaxin [40]. The C2 domains in dysferlin are also found in synaptotagmin VII, a Ca^{2+} sensor that when mutated results in an inflammatory disorder affecting skin and skeletal muscle [41]. Further implication of dysferlin in membrane repair is its reported interaction with AHNAK and annexin A2, both members of the membrane repair complex (reviewed in [39]).

Another corollary of Ca^{2+} sensing and vesicle endocytotic activities implicates dysferlin in muscle myotube fusion and the related protein, myoferlin, has been shown to regulate myoblast fusion [42]. More recently, dysferlin-null myoblasts were found to be less efficient in myotube fusion and show a decreased response to IGF-I-induced hypertrophy, suggesting that dysferlin's activity in membrane repair is also important for myotube fusion [29]. Our studies do not contradict the idea that interactions of dysferlin in membrane repair could reduce myofusion efficiency, but do suggest that activation of intrinsic inflammatory networks in dysferlin-deficient muscle cells interferes with myofusion and that both processes contribute to reduced myogenesis.

4.3. Is there defective muscle regeneration in dysferlinopathy?

A/J mice have smaller muscle cross sectional area, form smaller myotubes and accumulate smaller numbers of myonuclei [29]. However, whether regeneration is perturbed remains unclear. By some accounts, SJL/J mice on the C57Bl10 background also show regeneration defects in response to injury [30] but others report exemplary muscle regeneration in SJL/J mice [43,44] and efficient expression of MyoD and myogenin in culture. These discrepancies raise the possibility that strain-specific differences dominate the vigor of muscle regeneration. However, in the presented studies, myoblasts derived from two independent mouse models of dysferlin deficiency showed diminished myofusion, suggesting that the dysferlin-deficiency itself imposes a deficit that is attributable to intrinsic inflammatory activity.

A key difference between myogenesis in murine dysferlin-deficient myoblasts and human cultures is the degree of the myogenic defect. Myotube formation itself was not compromised in murine dysferlin-deficient cells, as has been reported for human muscle cultures [15]. Thus the more severe pathology in human LGMD2B compared with the mouse seems to parallel the more pronounced myofusion defect observed in primary human dysferlin-deficient myoblasts.

Characterization of regeneration in injured dysferlin-deficient muscle showed no major differences in expression of muscle specific genes including *Pax7* and *Myod in vivo* [30]. Furthermore, contraction-induced injury of dysferlin-deficient muscle results in increased macrophage infiltration and prolonged regeneration suggesting that dysferlin-deficient muscle fibers are more sensitive to injury than normal [45]. Together with our findings, these data demonstrate that absence of dysferlin does not render the muscle completely incapable of proliferation, differentiation and fusion into myofibers. However, our studies suggest that intrinsic factors within dysferlin-deficient muscle reduce the efficiency with which regeneration may occur.

4.4. Use of anti-inflammatory agents as treatment for dysferlinopathy

Use of anti-inflammatories as therapeutic targets in dystrophin- and dysferlin-deficiency has received considerable attention in the clinical field, although their efficacy in practice remains less clear. Antioxidants such as coenzyme Q10 and resveratrol decrease dystrophic markers and enhance tissue integrity in SJL/J mice [46]. It has also been suggested that overactive complement C3 could be partially responsible for the muscle pathology [47].

Celastrol, a triterpene derived from *Tripterygium regelii* (“Thunder of God Vine”), has been shown to contain potent anti-cancer and anti-inflammatory properties and reduce NFκB and TNFα signaling (reviewed in [48]). Celastrol is currently being investigated as a treatment for arthritis, Alzheimer’s disease, and several types of cancer including glioma and prostate cancer (reviewed in [48]). In tumor cell lines, celastrol inhibits TNFα-dependent IκBα degradation and IKK activation, and nuclear translocation of phosphorylated p65/RelA, suggesting that it exerts its activity by interfering with cytoplasmic kinase complexes [49]. In the C2C12 muscle cell line, celastrol inhibited TNFα-induced NFκB signaling more potently then several tested glucocorticoids including prednisolone [34]. In the present study, we show for the first time that using celastrol at concentrations that lead to potent blockade of NFκB signaling, improves myogenesis in dysferlin-deficient myoblasts. Whereas the glucocorticoid NFκB inhibitor dexamethasone has been previously shown to increase myotube size [16], restoration of myogenic activity by celastrol has not been tested previously. Future studies will compare the activities of other non-glucocorticoid NFκB blockers on muscle myogenesis. These studies support the idea of using anti-inflammatory strategies to ameliorate symptoms in inflammatory muscle disorders including LGMD2B and encourages our further pursuit of the potential benefits of anti-inflammatory agents for inflammatory muscle disorders including DMD and LGMD2B.

Acknowledgments

The authors thank Kanneboyina Nagaraju for helpful discussion. The project described was supported by the Jain Foundation and in part by Grant Number P50AR060836 from the National Institute of Arthritis and Musculoskeletal and Skin Diseases. The content is solely the responsibility of the authors and does not necessarily represent the official views of the National Institute of Arthritis and Musculoskeletal and Skin Diseases or the National Institutes of Health.

References

1. Liu J, Aoki M, Illa I, et al. Dysferlin, a novel skeletal muscle gene, is mutated in Miyoshi myopathy and limb girdle muscular dystrophy. Nat Genet. 1998; 20:31–6. [PubMed: 9731526]
2. Mahjneh I, Marconi G, Bushby K, Anderson LV, Tolvanen-Mahjneh H, Somer H. Dysferlinopathy (LGMD2B): a 23-year follow-up study of 10 patients homozygous for the same frameshifting dysferlin mutations. Neuromuscul Disord. 2001; 11:20–6. [PubMed: 11166162]
3. Bashir R, Strachan T, Keers S, et al. A gene for autosomal recessive limb-girdle muscular dystrophy maps to chromosome 2p. Hum Mol Genet. 1994; 3:455–7. [PubMed: 8012357]
4. Bushby KM. Making sense of the limb-girdle muscular dystrophies. Brain. 1999; 122(Pt. 8):1403–20. [PubMed: 10430828]
5. Linssen WH, Notermans NC, Van der Graaf Y, et al. Miyoshi-type distal muscular dystrophy. Clinical spectrum in 24 Dutch patients. Brain. 1997; 120(Pt. 11):1989–96. [PubMed: 9397016]
6. Illa I, Serrano-Munuera C, Gallardo E, et al. Distal anterior compartment myopathy: a dysferlin mutation causing a new muscular dystrophy phenotype. Ann Neurol. 2001; 49:130–4. [PubMed: 11198284]
7. Cenacchi G, Fanin M, De Giorgi LB, Angelini C. Ultrastructural changes in dysferlinopathy support defective membrane repair mechanism. J Clin Pathol. 2005; 58:190–5. [PubMed: 15677541]
8. Fanin M, Angelini C. Muscle pathology in dysferlin deficiency. Neuropathol Appl Neurobiol. 2002; 28:461–70. [PubMed: 12445162]
9. Anderson LV, Davison K, Moss JA, et al. Dysferlin is a plasma membrane protein and is expressed early in human development. Hum Mol Genet. 1999; 8:855–61. [PubMed: 10196375]
10. Laval SH, Bushby KM. Limb-girdle muscular dystrophies – from genetics to molecular pathology. Neuropathol Appl Neurobiol. 2004; 30:91–105. [PubMed: 15043707]
11. Davis DB, Delmonte AJ, Ly CT, McNally EM. Myoferlin, a candidate gene and potential modifier of muscular dystrophy. Hum Mol Genet. 2000; 9:217–26. [PubMed: 10607832]
12. Bansal D, Campbell KP. Dysferlin and the plasma membrane repair in muscular dystrophy. Trends Cell Biol. 2004; 14:206–13. [PubMed: 15066638]
13. Bansal D, Miyake K, Vogel SS, et al. Defective membrane repair in dysferlin-deficient muscular dystrophy. Nature. 2003; 423:168–72. [PubMed: 12736685]
14. Roche JA, Lovering RM, Bloch RJ. Impaired recovery of dysferlin-null skeletal muscle after contraction-induced injury in vivo. Neuro-report. 2008; 19:1579–84.
15. de Luna N, Gallardo E, Soriano M, et al. Absence of dysferlin alters myogenin expression and delays human muscle differentiation “in vitro”. J Biol Chem. 2006; 281:17092–8. [PubMed: 16608842]
16. Belanto JJ, Diaz-Perez SV, Magyar CE, et al. Dexamethasone induces dysferlin in myoblasts and enhances their myogenic differentiation. Neuromuscul Disord. 2010; 20:111–21. [PubMed: 20080405]
17. Klinge L, Laval S, Keers S, et al. From T-tubule to sarcolemma: damage-induced dysferlin translocation in early myogenesis. FASEB J. 2007; 21:1768–76. [PubMed: 17363620]
18. Rawat R, Cohen TV, Ampong B, et al. Inflammasome up-regulation and activation in dysferlin-deficient skeletal muscle. Am J Pathol. 2010; 176:2891–900. [PubMed: 20413686]
19. Luo G, Hershko DD, Robb BW, Wray CJ, Hasselgren PO. IL-1beta stimulates IL-6 production in cultured skeletal muscle cells through activation of MAP kinase signaling pathway and NF-kappa B. Am J Physiol Regul Integr Comp Physiol. 2003; 284:R1249–54. [PubMed: 12676746]

20. Sarkar A, Duncan M, Hart J, Hertlein E, Guttridge DC, Wewers MD. ASC directs NF-kappaB activation by regulating receptor interacting protein-2 (RIP2) caspase-1 interactions. J Immunol. 2006; 176:4979–86. [PubMed: 16585594]
21. Wang H, Hertlein E, Bakkar N, et al. NF-kappaB regulation of YY1 inhibits skeletal myogenesis through transcriptional silencing of myofibrillar genes. Mol Cell Biol. 2007; 27:4374–87. [PubMed: 17438126]
22. Peterson JM, Bakkar N, Guttridge DC. NF-kappaB signaling in skeletal muscle health and disease. Curr Top Dev Biol. 2011; 96:85–119. [PubMed: 21621068]
23. Guttridge DC, Mayo MW, Madrid LV, Wang CY, Baldwin AS Jr. NF-kappaB-induced loss of MyoD messenger RNA: possible role in muscle decay and cachexia. Science. 2000; 289:2363–6. [PubMed: 11009425]
24. Acharyya S, Villalta SA, Bakkar N, et al. Interplay of IKK/NF-kappaB signaling in macrophages and myofibers promotes muscle degeneration in Duchenne muscular dystrophy. J Clin Invest. 2007; 117:889–901. [PubMed: 17380205]
25. Peterson JM, Guttridge DC. Skeletal muscle diseases, inflammation, and NF-kappaB signaling: insights and opportunities for therapeutic intervention. Int Rev Immunol. 2008; 27:375–87. [PubMed: 18853344]
26. Morgan JE, Beauchamp JR, Pagel CN, et al. Myogenic cell lines derived from transgenic mice carrying a thermolabile T antigen: a model system for the derivation of tissue-specific and mutation-specific cell lines. Dev Biol. 1994; 162:486–98. [PubMed: 8150209]
27. Ho M, Post CM, Donahue LR, et al. Disruption of muscle membrane and phenotype divergence in two novel mouse models of dysferlin deficiency. Hum Mol Genet. 2004; 13:1999–2010. [PubMed: 15254015]
28. Pfaffl MW. A new mathematical model for relative quantification in real-time RT-PCR. Nucleic Acids Res. 2001; 29:e45. [PubMed: 11328886]
29. Demonbreun AR, Fahrenbach JP, Deveaux K, Earley JU, Pytel P, McNally EM. Impaired muscle growth and response to insulin-like growth factor 1 in dysferlin-mediated muscular dystrophy. Hum Mol Genet. 2011; 20:779–89. [PubMed: 21127009]
30. Chiu YH, Hornsey MA, Klinge L, et al. Attenuated muscle regeneration is a key factor in dysferlin-deficient muscular dystrophy. Hum Mol Genet. 2009; 18:1976–89. [PubMed: 19286669]
31. Millay DP, Maillet M, Roche JA, et al. Genetic manipulation of dysferlin expression in skeletal muscle: novel insights into muscular dystrophy. Am J Pathol. 2009; 175:1817–23. [PubMed: 19834057]
32. Weller AH, Magliato SA, Bell KP, Rosenberg NL. Spontaneous myopathy in the SJL/J mouse: pathology and strength loss. Muscle Nerve. 1997; 20:72–82. [PubMed: 8995586]
33. Bittner RE, Anderson LV, Burkhardt E, et al. Dysferlin deletion in SJL mice (SJL-Dysf) defines a natural model for limb girdle muscular dystrophy 2B. Nat Genet. 1999; 23:141–2. [PubMed: 10508505]
34. Baudy AR, Saxena N, Gordish H, Hoffman EP, Nagaraju K. A robust in vitro screening assay to identify NF-kappaB inhibitors for inflammatory muscle diseases. Int Immunopharmacol. 2009; 9:1209–14. [PubMed: 19596085]
35. Lu A, Proto JD, Guo L, et al. NF-kappaB negatively impacts the myogenic potential of muscle-derived stem cells. Mol Ther. 2012; 20:661–8. [PubMed: 22158056]
36. De Luna N, Gallardo E, Sonnet C, et al. Role of thrombospondin 1 in macrophage inflammation in dysferlin myopathy. J Neuropathol Exp Neurol. 2010; 69:643–53. [PubMed: 20467328]
37. Pang ZP, Sudhof TC. Cell biology of Ca^{2+}-triggered exocytosis. Curr Opin Cell Biol. 2010; 22:496–505. [PubMed: 20561775]
38. Idone V, Tam C, Andrews NW. Two-way traffic on the road to plasma membrane repair. Trends Cell Biol. 2008; 18:552–9. [PubMed: 18848451]
39. Han R. Muscle membrane repair and inflammatory attack in dysferlinopathy. Skelet Muscle. 2011; 1:10. [PubMed: 21798087]
40. Johnson CP, Chapman ER. Otoferlin is a calcium sensor that directly regulates SNARE-mediated membrane fusion. J Cell Biol. 2010; 191:187–97. [PubMed: 20921140]

41. Reddy A, Caler EV, Andrews NW. Plasma membrane repair is mediated by Ca(2+)-regulated exocytosis of lysosomes. Cell. 2001; 106:157–69. [PubMed: 11511344]

42. Doherty KR, Cave A, Davis DB, et al. Normal myoblast fusion requires myoferlin. Development. 2005; 132:5565–75. [PubMed: 16280346]

43. Mitchell CA, Grounds MD, Papadimitriou JM. The genotype of bone marrow-derived inflammatory cells does not account for differences in skeletal muscle regeneration between SJL/J and BALB/c mice. Cell Tissue Res. 1995; 280:407–13. [PubMed: 7781037]

44. Maley MA, Fan Y, Beilharz MW, Grounds MD. Intrinsic differences in MyoD and myogenin expression between primary cultures of SJL/J and BALB/C skeletal muscle. Exp Cell Res. 1994; 211:99–107. [PubMed: 8125164]

45. Roche JA, Lovering RM, Roche R, Ru LW, Reed PW, Bloch RJ. Extensive mononuclear infiltration and myogenesis characterize recovery of dysferlin-null skeletal muscle from contraction-induced injuries. Am J Physiol Cell Physiol. 2010; 298:C298–312. [PubMed: 19923419]

46. Potgieter M, Pretorius E, Van der Merwe CF, et al. Histological assessment of SJL/J mice treated with the antioxidants coenzyme Q10 and resveratrol. Micron. 2011; 42:275–82. [PubMed: 21036052]

47. Han R, Frett EM, Levy JR, et al. Genetic ablation of complement C3 attenuates muscle pathology in dysferlin-deficient mice. J Clin Invest. 2010; 120:4366–74. [PubMed: 21060153]

48. Kannaiyan R, Shanmugam MK, Sethi G. Molecular targets of celastrol derived from Thunder of God Vine: potential role in the treatment of inflammatory disorders and cancer. Cancer Lett. 2011; 303:9–20. [PubMed: 21168266]

49. Sethi G, Ahn KS, Pandey MK, Aggarwal BB. Celastrol, a novel triterpene, potentiates TNF-induced apoptosis and suppresses invasion of tumor cells by inhibiting NF-kappaB-regulated gene products and TAK1-mediated NF-kappaB activation. Blood. 2007; 109:2727–35. [PubMed: 17110449]

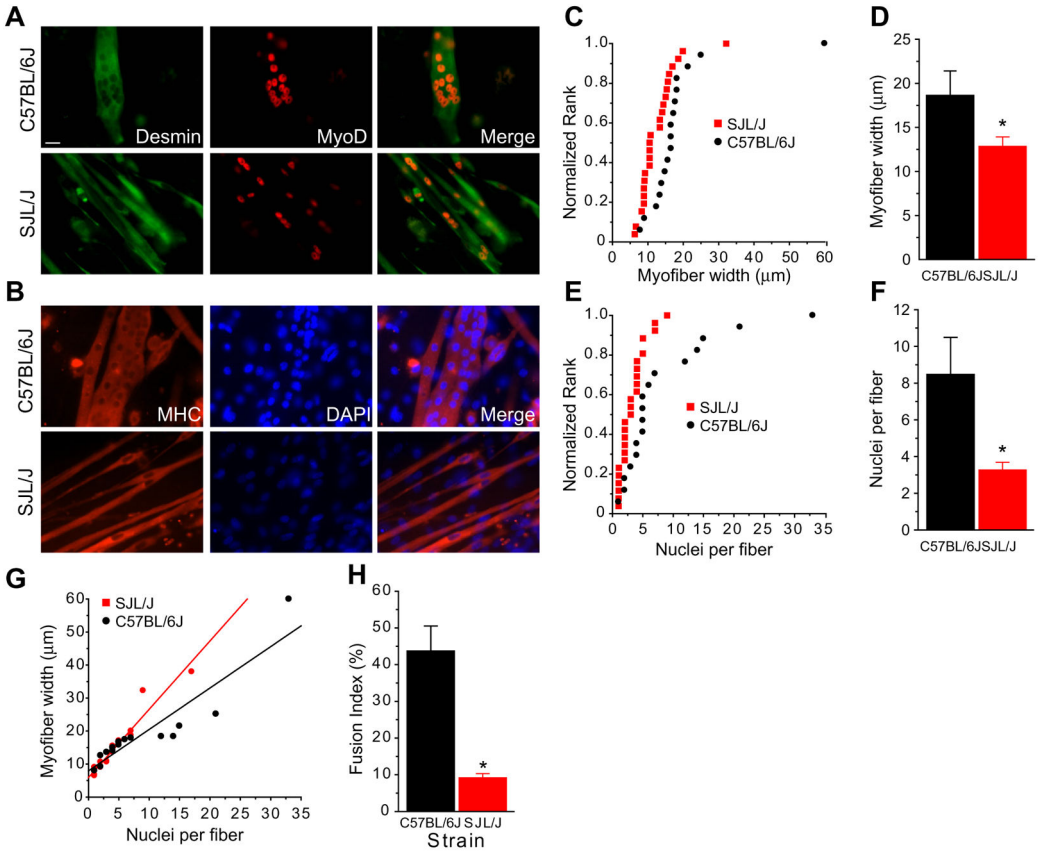

Fig. 1.

SJL/J muscle fuse to form myotubes in culture. (A and B) Muscle satellite cells were derived from SJL/J (left) or C57Bl/6J (right) mice, cultured for 7 days in growth media, then 2 days in fusion medium. Cultures were immunostained with anti-desmin (green) and MyoD (red) antibodies (A) or anti-MHC (red) and counterstained with DAPI (blue) (B). C57Bl/6J cells formed large-diameter fibers containing many nuclei, whereas SJL/J cells formed many thin fibers containing a few nuclei each. (C) Cumulative frequency distribution of myotube width plotted against normalized rank in tissue cultures of SJL/J and C57BL/6J muscle cells. Fiber diameters (*y*-axis) were quantitated in each of up to 26 muscle fibers of muscle cultures grown and differentiated as described above. Graph represents the range of fiber diameters (in microns) from SJL/J (black) and C57Bl/6J (red) cultures. (D) Summary data of (C), showing reduced myofiber width in SJL/J cultures compared to wild-type muscle cultures. (E) Cumulative frequency distribution of myotube nuclei number per fiber plotted against normalized rank in SJL/J and C57Bl/6J cultures. (F) Summary data of (E), showing reduced nuclei per fiber in SJL/J cultures compared to C57Bl/6J. (G) Plot of myotube width against myonuclear number, showing reduced numbers of nuclei per fiber and decreased fiber thickness for SJL/J derived muscle cultures. (H) Fusion index was decreased in SJL/J myotubes compared to C57Bl/6J. n = 202 SJL/J and 226 C57Bl/6J total nuclei counted in three fields; $^{*}P < 0.05$. Scale bar = 20 μm.

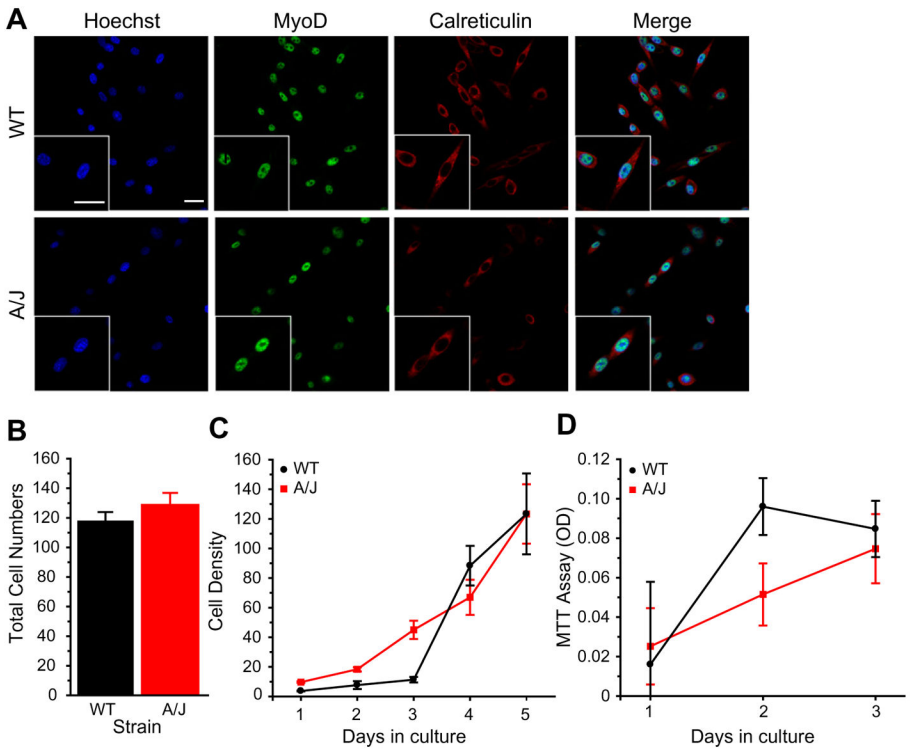

Fig. 2.

A/J deficient myoblasts do not show proliferation defects. (A) Dysferlin-sufficient (WT) and dysferlin-deficient (A/J) H-2K cells were plated at equal density and immunostained with indicated antibodies. (B) After 3 days in culture, total number of cells was counted. There was no significant difference in proliferation rates between A/J and WT H-2K cells. (C) Cell counts were taken after 5 days of culture in three independent A/J H-2K clones. There were no differences in proliferation. (D) MTT assay showing no differences in proliferation between A/J H-2K and WT cells. Scale bar = 25 μm.

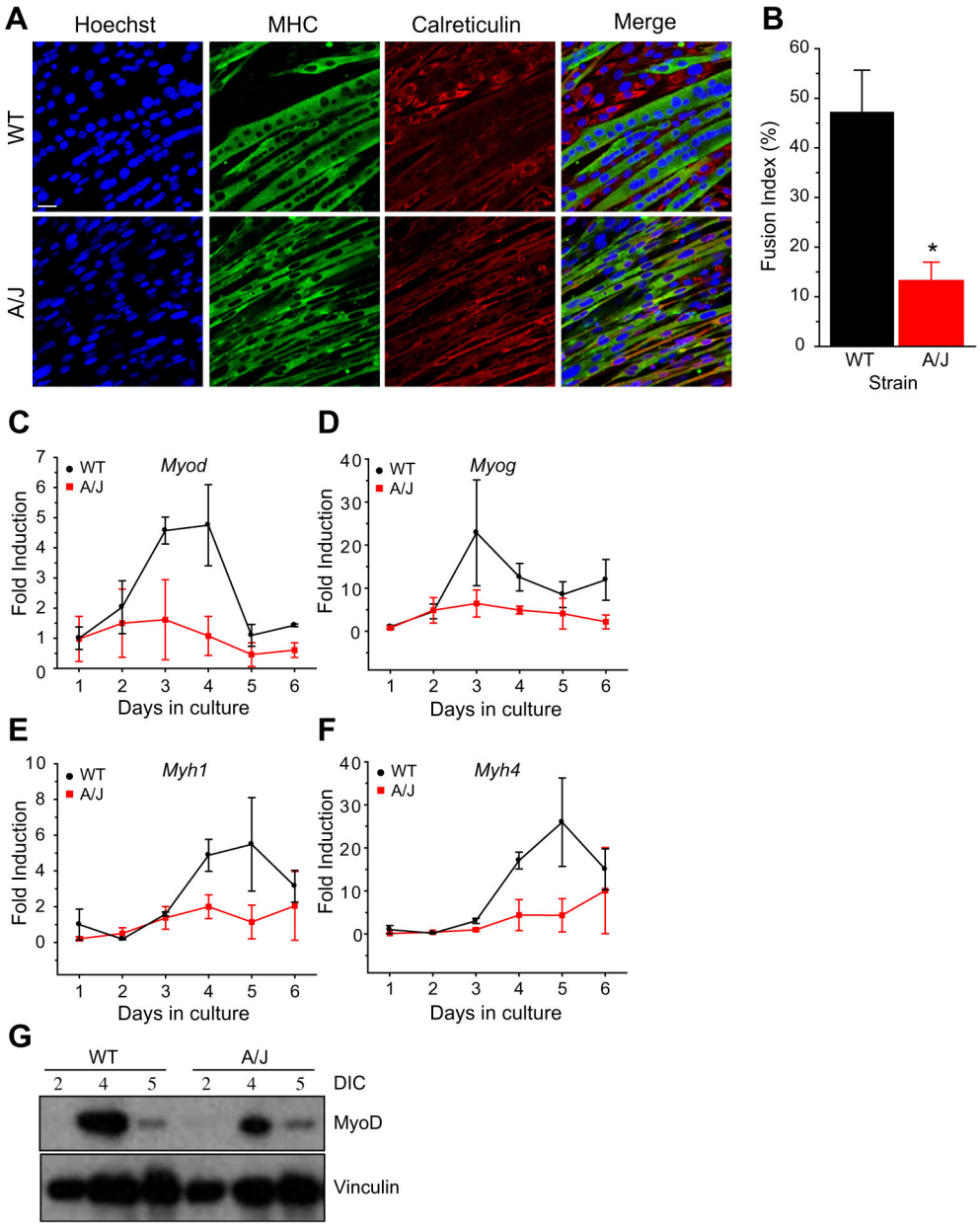

Fig. 3.

A/J myotubes form thinner myotubes and show a reduced myofusion index. (A) Immunostaining of A/J myotubes with antibodies for myosin heavy chain (MHC), calreticulin and Hoechst. (B) Quantitation of the fusion index. n = 386 (WT), 448 (A/J) total nuclei were counted containing 186 (WT) and 63 (A/J) myotubes in four non-overlapping fields. $P < 0.05$. (C–F) Real-time expression of myogenic genes during the time course of differentiation. Cultures from three independent H-2K A/J or WT clones were differentiated for up to 6 days in culture. Myogenic gene expression was measured using qPCR for MyoD (*Myod*) (C), myogenin (*Myog*) (D), myosin heavy chain 1 (*Myh1*) (E) and myosin heavy chain 4 (Myh4) (F). (G) Top: Western blot of MyoD expression between 2 and 5 days in

culture (DIC) in WT and A/J H-2K cells. *Bottom*: Vinculin was used as a protein loading control. Scale bar = 25 μm.

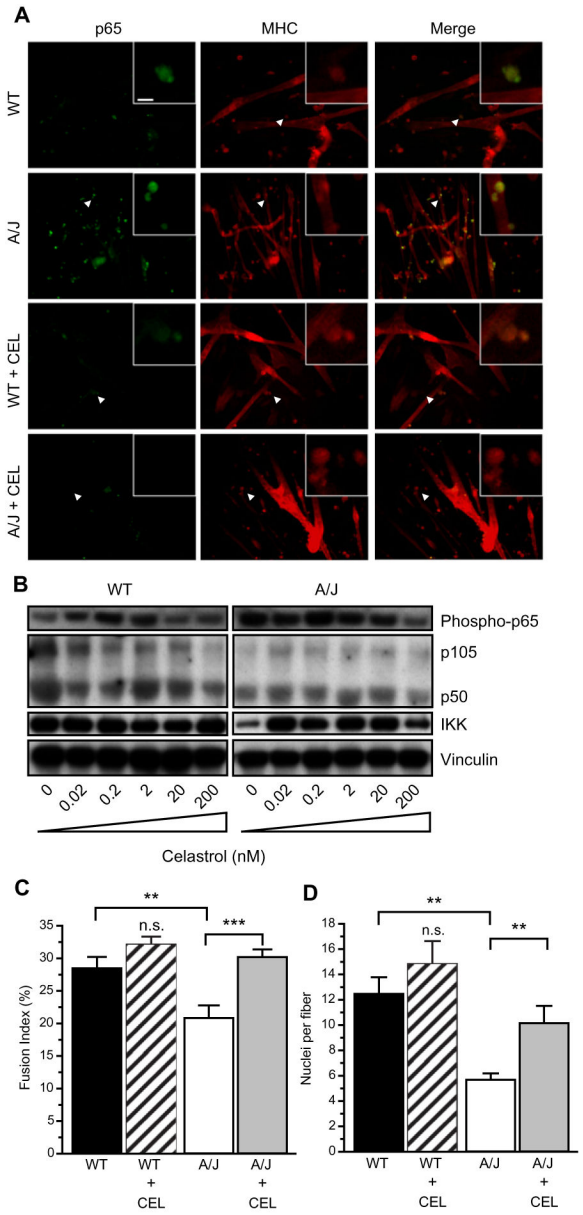

Fig. 4.

Celastrol blocks NFκB signaling. (A) Celastrol inhibits p65 activation and increases fiber diameters. Myoblasts were cultured in 6-well dishes. Twenty-four hours later, media was switched to differentiation media containing 200 nM celastrol. After 5 days in culture, myotubes were stained with antibodies to phospho-p65 (green) and anti-MHC (red). Phospho-p65 levels were higher in cultures of A/J cells compared to wild-type cells. Incubation of differentiating myoblasts with celastrol decreased phospho-p65 in the cultures and increased diameters of cells, shown with MHC staining. Inset shows higher magnification of area indicated by arrowhead. Scale bar = 20 and 5 μm in inset. (B) Cells were plated in 6-well dishes and celastrol was added at indicated concentrations after 24 h, the myotubes were harvested after 5 days. Western blot showing that phosphorylated p65 subunit of NFκB is upregulated in A/J cells and decreases with celastrol treatment (top).

Total expression of p105, p50, and IKK is not altered with celastrol treatment. (C and D) Fusion index and nuclei per fiber were calculated from six random fields in two independent experiments. Celastrol significantly increased fusion index (C) and nuclei per fiber (D) in A/J cultures. Scale bar = 20 μm. $^{**}P < 0.05$. $^{***}P < 0.01$.

Table 1

Upregulated genes in A/J myotubes compared to WT.

Gene symbol	Accession	Fold regulation	P-value	Description
CASP1	NM_009807	8.074	0.005283	Caspase 1; IL-1β converting enzyme
IKBKE	NM_019777	2.555	0.005499	Inhibitor of kappa light polypeptide gene enhancer I B-cells kinase epsilon (IKK-ε)
TNFSF14	NM_019418	1.8417	0.005601	Tumor necrosis factor ligand 14
RIPK1	NM_009068	1.4682	0.005616	TNFRSF-interacting serine–threonine kinase 1
IL1R1	NM_008362	1.3731	0.00641	Interleukin 1 receptor, type I
NFKBIA	NM_010907	1.4234	0.008922	Nuclear factor of kappa light polypeptide gene enhancer I B-cells inhibitor, alpha (IκBα)
MALT1	NM_172833	2.9197	0.010395	Mucosa associated lymphoid tissue lymphoma translocation gene 1
MAP3K1	NM_011945	1.3371	0.012835	Mitogen-activated protein kinase kinase kinase 1
BCL10	NM_009740	1.3743	0.014181	B-cell leukemia/lymphoma 10
IL1B	NM_008361	1.5819	0.020047	Interleukin 1 beta
AKT1	NM_009652	1.5422	0.022827	Thymoma viral proto-oncogene 1
TLR9	NM_031178	1.5148	0.035545	Toll-like receptor 9
JUN	NM_010591	1.5488	0.044134	Jun oncogene; activator protein 1
SLC44A2	NM_152808	1.3709	0.04511	Solute carrier family 44 member 2
RELB	NM_009046	1.4056	0.060459	Avian reticuloendotheliosis viral oncogene
CFLAR	NM_009805	1.421	0.071965	CASP8 and FADD-like apoptosis regulator
IRAK1	NM_008363	2.096	0.077476	Interleukin-1 receptor associated kinase
FASLG	NM_010177	1.4813	0.084698	Fas ligand (TNF superfamily member 6)
GJA1	NM_010288	3.9818	0.110953	Gap junction protein, alpha 1
FADD	NM_010175	1.6649	0.146432	Fas (TNFRSF6)-associated via death domain
TRIM13	NM_023233	1.3004	0.147326	Tripartite motif-containing 13
ICAM1	NM_010493	1.3983	0.153045	Intercellular adhesion molecule 1
ELK1	NM_007922	1.3561	0.159154	Member of ETS oncogene family
LPAR1	NM_010336	1.3657	0.159469	Lysophosphatidic acid receptor 1
HMOX1	NM_010442	2.5448	0.206157	Heme oxygenase (decycling) 1
TLR3	NM_126166	1.6474	0.212925	Toll-like receptor 3
LTA	NM_010735	1.3579	0.264798	Lymphotoxin A
TLR4	NM_021297	1.3579	0.264798	Toll-like receptor 4
TNFRSF1A	NM_011609	1.3579	0.264798	Tumor necrosis factor receptor superfamily member 1a
EDARADD	NM_133643	1.3122	0.274549	Ectodysplasin-A receptor-associated death domain
CSF2	NM_009969	1.8589	0.314809	Colony stimulating factor 2 (granulocyte–macrophage)
IFNB1	NM_010510	1.5772	0.431395	Interferon beta 1, fibroblast
IL6	NM_031168	1.428	0.505621	Interleukin 6
CCL2	NM_011333	1.4446	0.615915	Chemokine (C-C motif) ligand 2
TLR6	NM_011604	1.325	0.71502	Toll-like receptor 6
IFNG	NM_008337	1.3409	0.990221	Interferon gamma

qRT-PCR array of A/J H-2K and WT H-2K myotubes. Inflammatory genes from the array that were upregulated >1.3-fold were included and are shown with *P*-values.